JOURNAL OF VIROLOGY, July 2007, p. 6846–6857 Vol. 81, No. 13
0022-538X/07/$08.00+0 doi:10.1128/JVI.00069-07

In Vitro Analysis of Transneuronal Spread of an Alphaherpesvirus Infection in Peripheral Nervous System Neurons▽†

B. Feierbach,[1,2]* M. Bisher,[1] J. Goodhouse,[1] and L. W. Enquist[1]

Department of Molecular Biology, Princeton, New Jersey 08544,[1] and Lewis-Sigler Institute for Integrative Genomics, Princeton, New Jersey 08544[2]

Received 10 January 2007/Accepted 11 April 2007

The neurotropic alphaherpesviruses invade and spread in the nervous system in a directional manner between synaptically connected neurons. Until now, this property has been studied only in living animals and has not been accessible to in vitro analysis. In this study, we describe an in vitro system in which cultured peripheral nervous system neurons are separated from their neuron targets by an isolator chamber ring. Using pseudorabies virus (PRV), an alphaherpesvirus capable of transneuronal spread in neural circuits of many animals, we have recapitulated in vitro all known genetic requirements for retrograde and anterograde transneuronal spread as determined previously in vivo. We show that in vitro transneuronal spread requires intact axons and the presence of the viral proteins gE, gI, and Us9. We also show that transneuronal spread is dependent on the viral glycoprotein gB, which is required for membrane fusion, but not on gD, which is required for extracellular spread. We demonstrate ultrastructural differences between anterograde- and retrograde-traveling virions. Finally, we show live imaging of dynamic fluorescent virion components in axons and postsynaptic target neurons.

A striking property of neurotropic alphaherpesviruses is the controlled spread of infection into and out of the peripheral nervous system. Under certain circumstances, these viruses also exhibit the property of transneuronal spread: the capacity to infect chains of synaptically connected neurons. As a result, some alphaherpesviruses, such as pseudorabies virus (PRV) and herpes simplex virus, have been used by neuroanatomists to label neural circuitry in the peripheral and central nervous systems. In the past decade, the literature describing alphaherpesviruses to define the synaptic architecture of the brain has increased dramatically (10, 11). However, the mechanisms by which these viruses invade and spread in the nervous system are poorly understood. One major reason for this lack of understanding is that the primary system available for mechanistic analysis is the intact nervous system of a living animal, which is not easily amenable to manipulation. In this report, we describe a novel isolator chamber system that recapitulates all known properties of transneuronal spread. This facile in vitro system offers many advantages, including the opportunity to use a variety of imaging systems. Unlike the previously described tripartite ring system (6) or other Campenot chamber systems, the new system utilizes a single, nonseptated Teflon ring. Ganglion explants are plated, axons are extended, and then the Teflon ring is placed on top of the axons, capturing a subpopulation of axon shafts and growth cones. Dissociated neurons then are plated inside the chamber ring and allowed to form connections with the explant axon termini. In the previously described tripartite chamber system, axon guidance grooves were etched in the culturing surface to encourage a subpopulation of growing axons to grow into the other compartments. Unfortunately, guidance grooves cannot be etched on glass surfaces, thereby hampering live imaging techniques. However in this new application, axon guidance grooves are not required as the chamber is placed on top of already formed axons. Any surface suitable for growing axons can be used. In addition, since the axons do not have to penetrate under the barrier wall and are instead "captured" by the ring, the number of axons that contact the target neurons inside the chamber is greater and more easily controlled.

We made several key observations on transneuronal spread using the isolator chamber system. First, we have established that the system is leakproof and that in vitro transneuronal spread depends entirely on axonal integrity. Second, the attenuated vaccine strain PRV Bartha, known to spread only from post- to presynaptic neurons in a neural circuit but not in the opposite direction (27), likewise cannot spread from an infected explant to neurons in the isolator chamber. However, PRV Bartha spreads easily from neurons within the chamber to explant neurons outside the chamber. Third, transneuronal spread of PRV from the explant to neurons within the chamber does not require gD, a viral glycoprotein required for infection by extracellular particles, but does require gB, a viral protein required for membrane fusion. Fourth, the kinetics of transneuronal spread from the explant to neurons within the chamber is rapid and requires less than 16 h. Fifth, by transmission electron microscopy (TEM), we have shown that explant-mediated infection resulted in capsids enclosed within vesicles in both proximal (outside the chamber) as well as distal (within the chamber) regions of the explant axons. In contrast, infection of neurons inside the chamber results in distal capsids (outside the chamber) lacking an envelope. Finally, we show that this system is amenable to live imaging of virion components in axons undergoing transneuronal spread and have be-

* Corresponding author. Mailing address: 301 Schultz Building, Department of Molecular Biology, Princeton University, Princeton, NJ 08544. Phone: (609) 258-4990. Fax: (609) 258-1035. E-mail: becket@princeton.edu.

† Supplemental material for this article may be found at http://jvi.asm.org/.

▽ Published ahead of print on 25 April 2007.

gun to dissect the visible events in spread. Both live imaging and TEM data confirm that virions have different structures (presence or absence of an envelope), depending on their direction of spread.

MATERIALS AND METHODS

Cells and virus strains. The swine kidney epithelial cell line PK15 was purchased from the American Type Culture Collection (CCL-22). PK15 cells were cultured in Dulbecco's modified Eagle's medium supplemented with 10% fetal bovine serum and 1% penicillin–streptomycin. All PRV stocks were produced in the PK15 cell line. PRV stocks used in this report include PRV Becker, a virulent isolate; PRV Bartha, an attenuated vaccine strain (16); PRV151, which is PRV Becker with gG replaced by green fluorescent protein (GFP) (7); PRV152, which is PRV Bartha with gG replaced by GFP (14); and GS1236, which encodes gD-GFP and monomeric red fluorescent protein (mRFP)-YP26 fusion proteins (provided by G. Smith, Northwestern University) (1). The following PRV mutants in the PRV Becker background were used. PRV GS442 (a gD null mutant in which the GFP gene replaces the gD open reading frame) was provided by G. Smith (Northwestern University) and was grown in a gD-complementing cell line (22). PRV HHF2A (a gB null mutant) was grown in a gB-complementing cell line (LP64e3).

Antibodies and fluorescent dyes. The antibodies used in this report include mouse monoclonal antibody against PRV major capsid protein (made by Alex Flood at the Princeton Monoclonal Antibody Facility [used at 1:100]), rabbit antibodies against phosphorylated neurofilament H (SMI-31; Abcam [used at 1:400]), and nonphosphorylated neurofilament H (SMI-32; Abcam [used at 1:400]). All secondary Alexa fluorophores (used at 1:500), Alexa Fluor 568-phalloidin (used at 1:40), and the Hoechst 33342 nuclear dye (used at 1:20,000) were purchased from Molecular Probes.

Neuronal cultures. Detailed protocols for dissecting and culturing neurons are found in the article by Ch'ng et al. (5). Briefly, sympathetic neurons from the superior cervical ganglia (SCG) were dissected from E15.5-to-E16.5 pregnant Sprague-Dawley rats (Hilltop Lab Animals, Inc., Scottdale, PA) cut in half with dissection knives. Ganglia were plated either on top of a square of Aclar (Electron Microscopy Sciences, PA) within a 35-mm plastic tissue culture dish or directly into Mat-Tek glass-bottom dishes (http://www.glass-bottom-dishes.com/). Dishes (or Aclar) were serially coated with 500 g/ml of poly-DL-ornithine (Sigma Aldrich) diluted in borate buffer and 10 g/ml of natural mouse laminin (Invitrogen). The neuron culture medium consists of Dulbecco's modified Eagle's medium (Invitrogen) and Ham's F-12 (Invitrogen) in a 1:1 ratio. The serum-free medium was supplemented with 10 mg/ml of bovine serum albumin (BSA [Sigma Aldrich]), 4.6 mg/ml glucose (J. T. Baker), 100 μg/ml of holotransferrin (Sigma Aldrich), 16 μg/ml of putrescine (Sigma Aldrich), 10 μg/ml of insulin (Sigma Aldrich), 2 mM of L-glutamine (Invitrogen), 50 μg/ml or units of penicillin and streptomycin (Invitrogen), 30 nM of selenium (Sigma Aldrich); 20 nM of progesterone (Sigma Aldrich), and 100 ng/ml of nerve growth factor 2.5S (Invitrogen). Two days postplating, the neuronal cultures are treated with 1 μM of the antimitotic drug cytosine-D-arabinofuranoside (Sigma-Aldrich) to eliminate any nonneuronal cells. The neuron culture medium was replaced every 3 days, and cultures were kept in a humidified, CO_2-regulated, 37°C incubator. Six days postplating of SCG explants, a Teflon chamber (see below for details) was placed adjacent to the explant to capture axons and their growth cones. Seven days postplating of SCG explants, dissociated SCG were placed inside the Teflon chamber. Dissociated SCG were incubated in 250 μg/ml of trypsin (Worthington Biochemicals) for 10 min. Trypsin inhibitor (1 mg/ml [Sigma Aldrich]) was added to neutralize the trypsin for 3 min and then removed and replaced with neuron culture medium. Prior to plating, the ganglia were triturated into dissociated neurons using a fire-polished Pasteur pipette and then plated in the Teflon ring placed within a 35-mm plastic tissue culture dish. Two days postplating, the neuronal cultures were treated with 1 μM of cytosine-D-arabinofuranoside. All experimental protocols related to animal use have been approved by The Institutional Animal Care and Use Committee of the Princeton University Research Board under protocol no. 1453-AR2, in accordance with the regulations of the American Association for Accreditation of Laboratory Animal Care and those in the Animal Welfare Act (Public Law 99-198).

Chamber culture system. Teflon rings were purchased from Tyler Research (Alberta, Canada), and protocols were modified from previously published reports for Campenot chambers (4, 6). Briefly, all of the tools and reagents including the Teflon rings and silicone grease-loaded syringe (Dow Corning) were sterilized via autoclaving prior to assembly. A 10-ml disposable syringe attached to a truncated P200 pipette tip was filled with silicone grease. Using the silicone grease-loaded syringe, a thin, continuous strip of silicone grease was applied over the entire bottom surface of a Teflon ring. The silicone grease-coated ring was placed into the medium and gently dropped over the 1-week old explant axons, adjacent to the explant cell bodies. The ring was allowed to settle by gravity over the axons and make contact with the surface of the Aclar for 24 h. The following day, dissociated superior cervical ganglia neurons (approximately one-fourth of a single ganglion, which results in about 5,000 cell bodies) were placed inside the ring. Neuron cultures were maintained according to established protocols stated in the previous section.

Assaying transneuronal spread of infection. Neuronal explants were cultured for 2.5 weeks in the trichamber system with frequent medium changes. Dissociated neurons inside the ring were cultured for 1.5 weeks. Neuron medium containing 1% hydroxypropyl methylcellulose (Methocel) was placed inside the chamber. The viral inoculum was diluted in neuron medium and added to the dish outside of the chamber. We routinely use a high multiplicity of infection (MOI) to infect all neurons and to overcome nonspecific adsorption of inoculum to the coated tissue culture dish. After 1 h, the unadsorbed viral inoculum was removed and replaced with neuron medium containing 1% hydroxypropyl methylcellulose. The chambers were incubated in a humidified 37°C incubator until the appropriate time, when the neurons were processed for immunofluorescence, titer determination, or live imaging. To determine the titer, the neurons inside the chamber were gently scraped from the dish with a pipette tip. The medium from inside the chamber was removed and frozen. The thawed aliquot was serially diluted, and the titer was determined on PK15 cells.

Indirect immunofluorescence. The explants were grown on the surface of a flexible thermoplastic fluoropolymer film known as Aclar (EM Sciences). Aclar is biochemically inert and exhibits no detectable autofluorescence. The Aclar was cut into squares that fit inside a 35-mm plastic tissue culture dish and UV sterilized for 20 min. After sterilization, the Aclar squares were coated with poly-DL-ornithine and laminin, and SCG explants were plated directly upon the Aclar surface. All subsequent neuron culture and viral infection protocols are similar to those described in previous sections. To fix the neurons both inside and outside the chamber, the medium was carefully removed, washed with phosphate-buffered saline (PBS), and replaced with 4% paraformaldehyde in PBS. Neurons were fixed for 10 min in the dark. After fixation, the chamber was carefully lifted from the Aclar and the remaining silicone grease was gently cleared without disrupting the fixed cells. The Aclar surface was then washed with PBS, followed by PBS containing 3% bovine serum albumin (BSA), and permeabilized by PBS with BSA and 0.5% Triton X-100 for 3 to 5 min. After permeabilization, primary antibodies were added for 1 h. After primary antibodies were removed, the sample was washed three times with PBS with BSA and 0.5% saponin. Next, secondary antibodies were added to the sample and incubated for 1 h. After 1 h, the secondary antibodies were removed and the sample was washed three times with PBS with BSA and 0.5% saponin. Following secondary antibody application, the samples were stained with Hoechst 33342 dye (1:20,000) for 10 min followed by three washes with PBS with BSA and 0.5% saponin. Samples on Aclar were mounted on a glass slide using Aqua Poly/Mount (Polysciences), and a coverslip was placed on top of the sample. The slide was air dried for 24 h prior to imaging.

Wide-field confocal microscopy and live imaging. Wide-field epifluorescence microscopy was performed with a Nikon Eclipse TE 2000-U microscope equipped with a Cooke SensiCam high-performance camera. Images were acquired using IP Lab software (Scanalytics, Inc.). The 2× and 4× fluorescence and bright-field images were acquired on a Leica MZFLIII stereomicroscope using a Jenoptik ProgRes C14 camera. Samples were imaged with a Perkin-Elmer RS3 spinning disk confocal microscope side-mounted on a TE200-S Nikon Eclipse microscope with an argon/krypton laser producing excitation lines of 488, 568, and 647 nm. Optical sections were acquired in 0.5-μm steps. Two-dimensional projections of confocal stacks and channel merges were created by ImageJ 1.37j software (National Institutes of Health). Live imaging was performed on the Leica SP5 with an HCX Plan Apochromat 63× 1.3 NA glycerin 37° UV objective at zoom factor 3. Prior to imaging, 25 mM HEPES was added to the medium. For live imaging experiments, neurons were cultured on MatTek Corp. glass-bottom dishes (http://www.glass-bottom-dishes.com/). The dish was warmed to 35°C employing a DH40i Micro-incubation system (Warner Instrument Corp.) run at constant voltage. Laser lines at 488 and 561 nm were used for simultaneous GFP and RFP excitation, with emissions from 495 to 553 nm and 587 to 702 nm collected for GFP and RFP, respectively. Images were acquired employing a 2.5-Airy-unit detector pinhole and scanning at a speed of 1,000 Hz in a bidirectional mode. For three-dimensional (3D) imaging over time (see Fig. 9), four 512-by-512 optical slices at 0.6-μm *z*-axis intervals were collected at each time point, providing a 1.28-s time interval per frame. Postacquisition, a 3-by-3 kernel median filter was applied to the data and a single 3D maximum projection

was performed at each time point. All figures were assembled in Adobe Photoshop 7.0.1. Alterations to image brightness and contrast were conducted in a linear manner and were applied equally to controls, except where otherwise noted.

Electron microscopy. The chamber was assembled on Aclar (EM Sciences) as described above. Cell bodies were infected at a high MOI, as described above, and after 16 h, the chambers were washed twice with PBS, fixed with 2% glutaraldehyde in 0.2 M sodium cacodylate buffer (pH 7.2) for 4 h, and postfixed with 1% osmium tetroxide in sodium veronal buffer for 1 h on ice. Samples were then rinsed with sodium veronal buffer four times and incubated with 0.25% toluidine blue in 0.2 M cacodylate buffer (pH 7.2) for 1 h; the staining solution was then removed with four rinses of sodium veronal buffer (pH 7.2), followed by four rinses with 0.05 M sodium maleate buffer (pH 5.1). Overnight incubation with 2% uranyl acetate in 0.05 M sodium maleate buffer was done in the dark followed by four rinses with 0.05 M sodium maleate buffer (pH 5.1). The fixed samples were then dehydrated with ethyl alcohol, embedded in Epon resin (EM Sciences), and cut into 70-nm sections using a Reichert Ultracut E ultramicrotome. Sections were obtained from both inside and outside the chamber and examined using a Leo 912AB transmission electron microscope operated at 80 kV. Removal of the chamber from the Aclar leaves behind a visible layer of grease that serves as a chamber "footprint." This mark aids in determining areas inside and outside the chamber wall.

RESULTS

Basics of the transneuronal culture system. The key components of the transneuronal system are shown in Fig. 1A. As described in Materials and Methods, one half of an SCG explant was plated in a 35-mm dish and a radial array of neurites grew from the explant. SCG are sympathetic peripheral nervous system ganglia that yield homogeneous neuronal populations in culture (3). In culture, SCG neurons maintain their electrophysiological properties and form synapses upon one another (3). After 1 week in culture, a Teflon ring was placed on top of the neurites, capturing a subpopulation of the neurites. The ring was lined with a thin ribbon of silicone grease and placed into the medium (grease-side down) and allowed to settle onto the dish by gravity. The ring did not harm the neurites as they continued to grow at the same pace (0.5 mm/day) after placement of the ring (data not shown). After 24 h, dissociated SCG neurons were plated inside the rings. The number of dissociated neurons was equivalent to ~25% of a ganglion. After 1.5 weeks in culture, the neurons inside the chamber ring were mature as shown by the cell-body-specific staining of nonphosphorylated neurofilament H and the exclusively axonal staining of phosphorylated neurofilament H (Fig. 1B). Both the axons emanating from the explant outside the chamber and the axons of dissociated neurons inside the chamber grew in parallel arrays, as shown by actin staining (Fig. 1C). This parallel axonal growth, rather than overlapping, crossing axons, allows one to follow (i.e., trace) individual axons and greatly facilitates tracking virus during live imaging. The neurons within the ring produce functional axons, as demonstrated by labeling with FM4-64, a fluorescent marker for firing neurons and intact axon termini (data not shown).

Spread of infection occurs from cell bodies outside the chamber to target neurons within the chamber. To determine if this chamber system could be used to study viral transneuronal spread, we infected the explant outside the chamber with PRV. Six chambers were assembled as described in Materials and Methods, and the explants were infected with PRV151, a PRV recombinant expressing a freely diffusible GFP at the gG locus. After 24 h after infection, the neurons both inside and outside the chamber were fixed and scored for the presence of

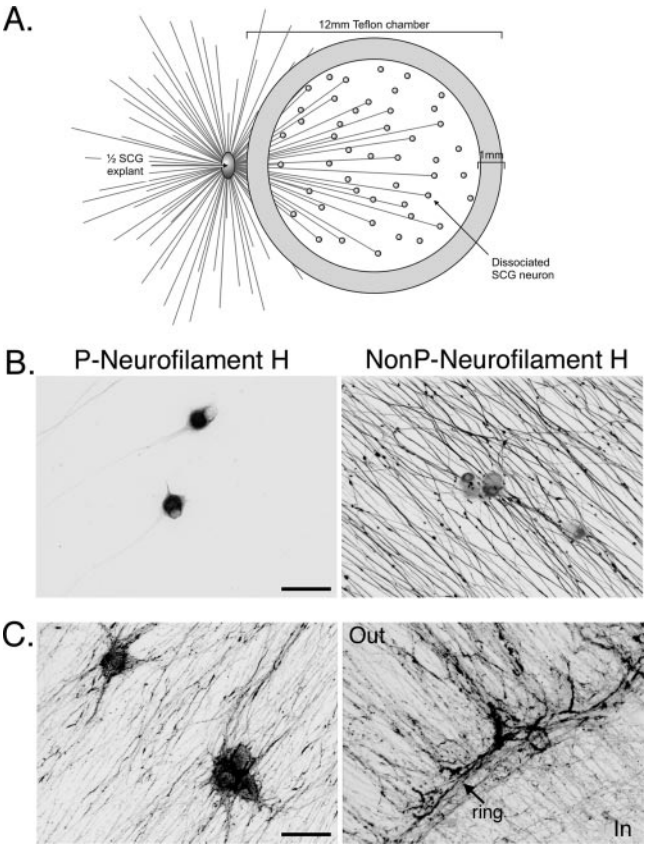

FIG. 1. Isolator chamber culture system. (A) The system consists of a 12-mm Teflon chamber ring placed on top of the axons emanating from half of an SCG explant. Dissociated SCG neurons are plated inside the culture ring, contacting the axons from the explant. (B) Dissociated SCG neurons cultured inside the ring are mature after 1.5 weeks. Shown are confocal microscopy images of dissociated SCG neurons inside the ring fixed and stained for phosphorylated (P) neurofilament H (left panel) and nonphosphorylated (NonP) neurofilament H (right panel). In mature neurons, phosphorylated neurofilament H is restricted to the cell body and nonphosphorylated neurofilament H is restricted to axons. Scale bar, 50 μm. (C) Confocal images of dissociated SCG neurons inside the ring (left) and the edge of the ring (right) stained for F-actin with AlexaFluor 568-phalloidin. "Out" and "In" denote the outside and inside of the ring, respectively, and an arrow points out the ring border. Scale bar, 50 μm.

GFP fluorescence. Both the explant outside the chamber (Fig. 2, large green fluorescent dot to left of chamber) and the individual neurons inside the chamber exhibited GFP fluorescence (Fig. 2 [each small green fluorescent dot inside chamber is a cell body]), demonstrating that PRV replicated in the cell bodies of the explant and the infection spread to the neurons inside the chamber. These green fluorescent dots inside the chamber were verified to be cell bodies under higher magnification. Inside the chamber, the number of cells containing GFP fluorescence decreased with increased distance from the explant, revealing a linear gradient of infection inside the chamber (data not shown). Had random leakage occurred, a radial gradient of infection should result, with fewer neurons infected at the center of the chamber. However, the infection gradient was linear, as predicted for transneuronal spread rather than diffusion of virus under the chamber barrier.

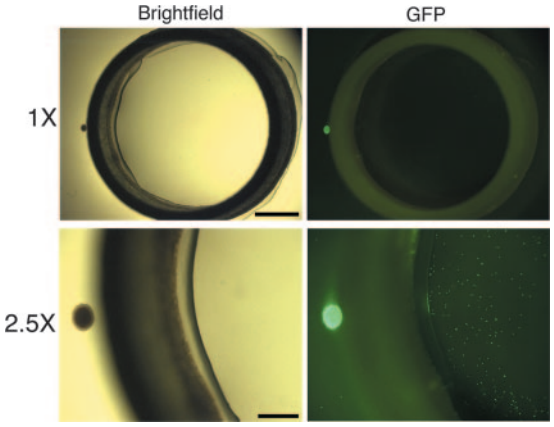

FIG. 2. Anterograde transneuronal spread of PRV in the isolator chamber system. The explants were infected with PRV151, a recombinant expressing GFP, and fixed at 24 h postinfection. Scale bar, 1 mm. The top panels are 1× wide-field images of the isolator chamber system, showing the relative size of the SCG explant (small dot on left side of ring) and the Teflon ring. The bottom panels are 2.5× wide-field images showing the explant as a large GFP-positive dot to the left side of the ring and dissociated neurons inside the ring as small GFP-positive dots. Scale bar, 0.5 mm.

Transneuronal spread of infection requires intact axons. We confirmed that axons were required for spread from explant neurons to second-order neurons within the chamber, rather than leakage under the chamber barrier, as follows. We infected explant neurons and then severed the axons to block transport to neurons within the chamber. We infected six chambers with PRV151 and added the inoculum to the outside of the chamber. For half of the chambers, we physically severed the axons between the explant and the chamber ring with a scalpel upon removal of the virus inoculum after 1 h of incubation. The remaining chambers were left untreated. After 24 h after infection, we monitored the GFP fluorescence inside the chamber. The spread of infection is completely blocked by physically severing axons from their cell bodies (Fig. 3). In addition, we harvested the neurons from the inside of the chamber and determined the titers of the contents on PK15 cells. We detected no plaques from the samples with severed axons (data not shown). From these results, we conclude transneuronal infection requires intact axons.

PRV Bartha is defective in anterograde transneuronal spread of infection. PRV Bartha is an attenuated virus defective in anterograde spread from presynaptic neurons to postsynaptic neurons in a variety of animal models (reviewed in reference 12). However, infection can spread readily from postsynaptic to presynaptic neurons (retrograde). For this reason, PRV Bartha is widely used to trace neuronal circuits (11). This remarkable directional spread phenotype primarily reflects the consequences of a small deletion that removes all or some of the coding sequences for gE, gI, and Us9 (15, 16, 18, 26, 33). We tested if PRV Bartha exhibited the same transneuronal directional spread phenotype observed in infection of neural circuits in animal models as well as the defect seen in neuron-to-cell spread in the in vitro trichamber system (6). We infected the SCG explant outside the chamber with PRV Bartha and PRV Becker, in parallel. After 24 h, neurons both inside and outside the chamber were fixed and stained with anti-VP5 (capsid) antibody and Hoechst stain to detect neuronal nuclei. As expected, PRV Becker infected the explant as well as the target neurons inside the chamber (Fig. 4A [explant not shown]). In contrast, PRV Bartha infected the explant but failed to spread to the neurons inside the chamber (Fig. 4A [explant not shown]). When we measured the degree of spread by scoring the number of VP5-positive cells ($n = 3$ chambers, 100 cells scored/chamber), we failed to find a single cell in the chambers infected with PRV Bartha that exhibited VP5 fluorescence (Fig. 4B). In contrast, PRV Becker spread to an average of 85% of the cells counted inside the chamber ($n = 3$ chambers, 100 cells scored/chamber; Fig. 4B).

A sensitive measure of the degree of infection is the yield of infectious particles. Accordingly, we harvested the neurons from inside the chamber at 24 h and determined the number of infectious particles on PK15 cells. We detected plaques only in the PRV Becker-infected neurons (Fig. 4C) and not in PRV Bartha-infected neurons. Even with the sensitive plaque assay method, we were unable to detect any spread of PRV Bartha from presynaptic to postsynaptic neurons.

Transneuronal spread requires gB but not gD. Next, we tested whether transneuronal spread occurs via direct neuron-

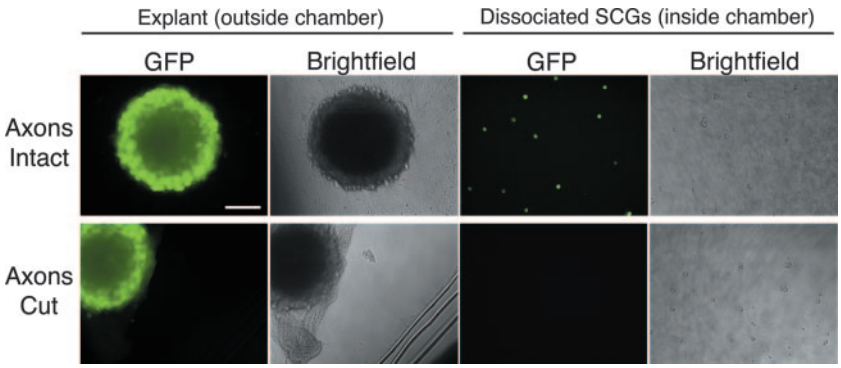

FIG. 3. Transneuronal spread of PRV in the isolator chamber system requires intact axons. The explants were infected at a high MOI with PRV151, a recombinant expressing GFP, and fixed at 24 h postinfection. When the axons are intact (top row), infection of the explant outside the chamber results in GFP-positive dissociated cells inside the chamber. When the axons are severed with a scalpel between the explant and the chamber (see cut marks in the dish in the bright-field image, bottom row), the dissociated cells inside the chamber are not infected (not GFP positive). All images are wide-field. Scale bar, 100 μm.

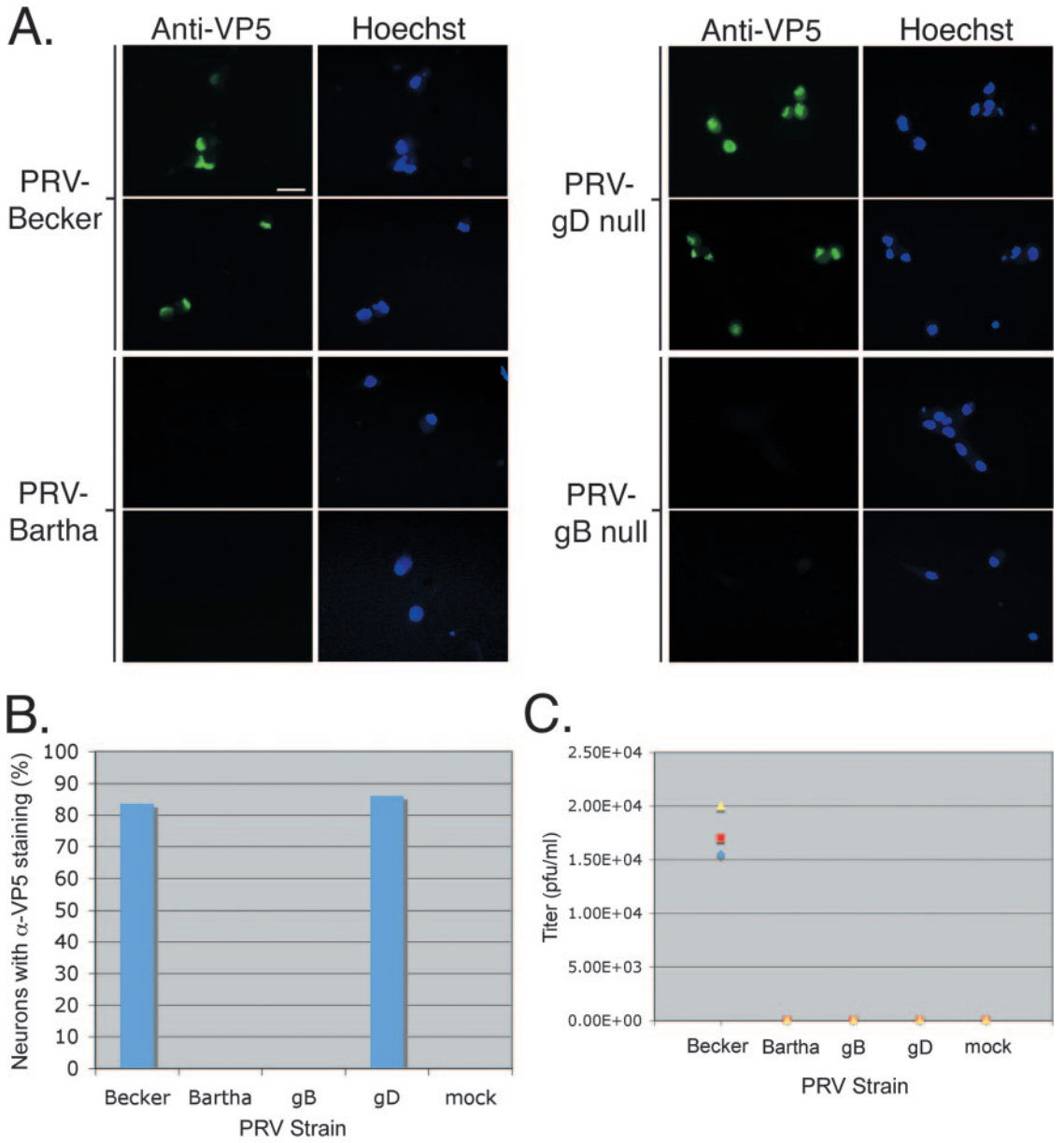

FIG. 4. Viral genetic requirements of in vitro transneuronal spread. Explants were infected with PRV Becker, PRV Bartha, GS442 (a complemented gD null virus that expresses GFP), or HF22A (a complemented gB null virus). (A) Wide-field images of neurons that are fixed and stained with anti-VP5 antibody and Hoechst 33342 at 24 h postinfection. Only dissociated cells inside the chamber are shown. The same field of neurons is shown in the anti-VP5 panel as in the Hoechst panel. Three chambers were used for each PRV strain. (B) Quantitation of neurons infected inside chambers. Neurons positive for anti-VP5 (α-VP5) staining were scored as infected. (C) Quantitation of spread via titer determination. The medium in the chamber was harvested at 24 h postinfection, and the titer was determined for PRV plaques on PK15 cells. Three chambers were used for each PRV strain. Scale bar, 20 μm.

neuron interaction or by infectious free virions. For PRV, the viral envelope protein gD is absolutely required for infection mediated by extracellular virions; however, PRV gD is not required for direct cell-to-cell spread of infection in vitro and in vivo (2, 6, 21, 24, 28). We infected the explant outside the chamber ring with PRV GS442, a gD null mutant that expresses GFP. We produced infectious PRV GS442 by growing virus stocks on a gD-expressing cell line. Complemented viruses can infect once, but the resulting progeny do not contain gD, and hence these gD null extracellular particles are noninfectious. We then infected the explants outside the chambers with the complemented PRV gD null mutant. Neurons both inside and outside the chamber were fixed and stained with anti-VP5 antibody and Hoechst 33342, a DNA stain. By direct fluorescence of GFP or by immunofluorescence, we could easily detect infected neurons inside the chamber (Fig. 4A). In fact, when we counted the number of VP5-positive cells inside the chamber of the gD mutant infection and compared it to that of PRV Becker, the numbers of plaques were similar (Fig. 4B; $n = 3$ chambers). However, when we harvested the neu-

rons from inside the chamber and determined their titers on PK15 cells, we could not detect any plaques on PK15 cells (Fig. 4C). Any progeny of virus that replicated in the explant and the chamber would not contain gD, and as a result, these extracellular particles are noninfectious. In addition, the absence of any plaques indicates there were no gD-positive revertants in the gD mutant stocks. We conclude that gD-mediated events are not required for transneuronal spread.

The viral gB protein is an essential glycoprotein required for transmission of infection either by extracellular particles or by cell-to-cell spread. In all in vivo and in vitro models tested so far, loss of gB renders particles completely noninfectious and no spread of infection occurs to adjacent cells (23, 28). This highly conserved viral protein is essential for the replication of all alphaherpesviruses tested (23, 28). We confirmed that gB is absolutely required for transneuronal spread of infection in the isolator chamber system. gB null mutant virus (PRV HF22A) stocks were grown in a cell line expressing full-length gB. Like a complemented gD mutant, a complemented gB mutant can infect only once and all of its subsequent progeny are noninfectious since they do not express gB. We infected the explants outside the chambers with the complemented PRV gB null virus. Neurons both inside and outside the chamber were fixed and stained with anti-VP5 antibody and Hoechst 33342. In contrast to the PRV gD null mutant, the gB null mutant infected only primary cells and failed to spread from the explant to the neurons inside the chamber. We could not detect any neurons inside the chamber that stained for VP5 (Fig. 4A and B). As expected, we detected no plaques on PK15 cells from neurons harvested inside the chamber (Fig. 4C). The absence of infectious virus and anti-VP5 signal inside the chambers confirms the failure of the gB null mutant to spread transneuronally.

Infection from primary neurons in the explant to the second-order neurons within the chamber is rapid. We characterized the kinetics of viral spread in the transneuronal chamber system by determining the length of time for virus to replicate in the explant, undergo axonal transport, and infect second-order neurons. We infected the explant with PRV Becker, monitoring viral spread every 4 h over a 24-h period. At each time point, neurons were fixed and stained with anti-VP5 antibody and Hoechst 33342. At 4 and 8 h after infection, infection was observed in the explant but had not spread to the neurons inside the chamber, as indicated by the lack of anti-VP5 fluorescence (Fig. 5A and B; $n = 3$ chambers/time point, 100 cells counted/chamber). By 12 h after infection, the infection had spread to a few cells inside the chamber, which exhibited anti-VP5 staining (Fig. 5A and B). However, by 16 h after infection, a significant number of infected cells were easily detected inside the chamber, with over 70% of the cells in the chamber exhibiting anti-VP5 staining (Fig. 5A and B; $n = 3$ chambers/time point, 100 cells counted/chamber). By 20 and 24 h after infection, the number of cells inside the chamber appeared to peak at approximately 85%, approximating the previous data set (Fig. 5A and B, compared with Fig. 4A, Becker). We most likely do not achieve 100% infection of cells inside the chamber because not all cells inside the chamber are synaptically connected to the explant outside the chamber wall. In parallel, we harvested the neurons from inside the chamber and determined the titers of infectious particles on PK15 cells. No plaques were detected from the 0-, 4-, and 8-h time points (Fig. 5C). Plaques were first detected at 12 h after infection, and the number increased thereafter (Fig. 5C). Thus, anterograde spread of PRV from primary neurons outside the chamber to secondary neurons inside the chamber occurs rapidly and in a fairly synchronous manner.

Transneuronal spread can occur in the retrograde direction. In our previous experiments, we demonstrated that the isolator chamber can be used to recapitulate anterograde transneuronal spread. We next determined if the system could be used to study retrograde transneuronal spread (spread from neurons inside the chamber to neurons outside). We infected three chambers in parallel with either PRV Becker (PRV151) or PRV Bartha (PRV152), each a recombinant strain expressing a freely diffusible GFP. At 24 h, both PRV Becker and PRV Bartha spread from the neurons inside the chamber to neurons in the explant outside of the chamber (Fig. 6). Importantly, PRV Bartha, which was unable to spread from explant neurons to secondary neurons in the chamber (Fig. 4), was fully capable of spreading to the explant neurons; thus, the directional spread defect of PRV Bartha can be completely recapitulated using the isolator chamber and SCG neurons.

Analysis of capsid structures in axons by TEM. Due to its defined geometry, the isolator chamber system provides useful opportunities for TEM. To demonstrate the method, we first infected neurons outside the chamber and analyzed capsid structures in axons inside the chamber wall. We found that capsids in axons are enclosed within vesicles (see enlarged images in Fig. 7, top row). These particles, located mid-axon, were generally single capsids enclosed within an intact membrane. These virions measured an average diameter of 215 ± 16 nm ($n = 40$ virions). Although we cannot determine if these axons emanate from the explant or from the dissociated neurons inside the chamber, given the time after infection (20 h), it is likely that the capsid structures were produced in explant neurons and have moved into the chamber by anterograde transport mechanisms. We also examined axons outside the chamber wall proximal to the explant and found that all capsids were within membranes as well. In addition, we observed capsids with similar structures in chambers without target neurons (B. Feierbach, M. Bisher, and L. Enquist, unpublished data). We conclude that during viral egress via axons, PRV capsids are transported in cellular membranes. The nature of these viral particles, as well as the origin of the cellular membrane, remains to be determined.

We also determined the structure of capsids after primary infection of axons. We infected dissociated neurons inside the chambers with PRV Becker for 20 h and fixed and prepared the samples for TEM. We looked for capsids in axons outside the chamber wall, proximal to the explant. In contrast to the progeny capsids in axons traveling in the anterograde direction, infecting capsids in axons prior to replication were not found in vesicles (Fig. 7, bottom row). Instead, we observed only "naked" capsids surrounded by a halo of electron-dense material, possibly tegument proteins. The dark center of these virions measured an average of 93 ± 7 nm across ($n = 45$ virions), the same size as previously reported for capsids (32). We also examined PRV Bartha capsids early after axonal infection. Although fewer capsids were observed, they were "naked" and not trans-

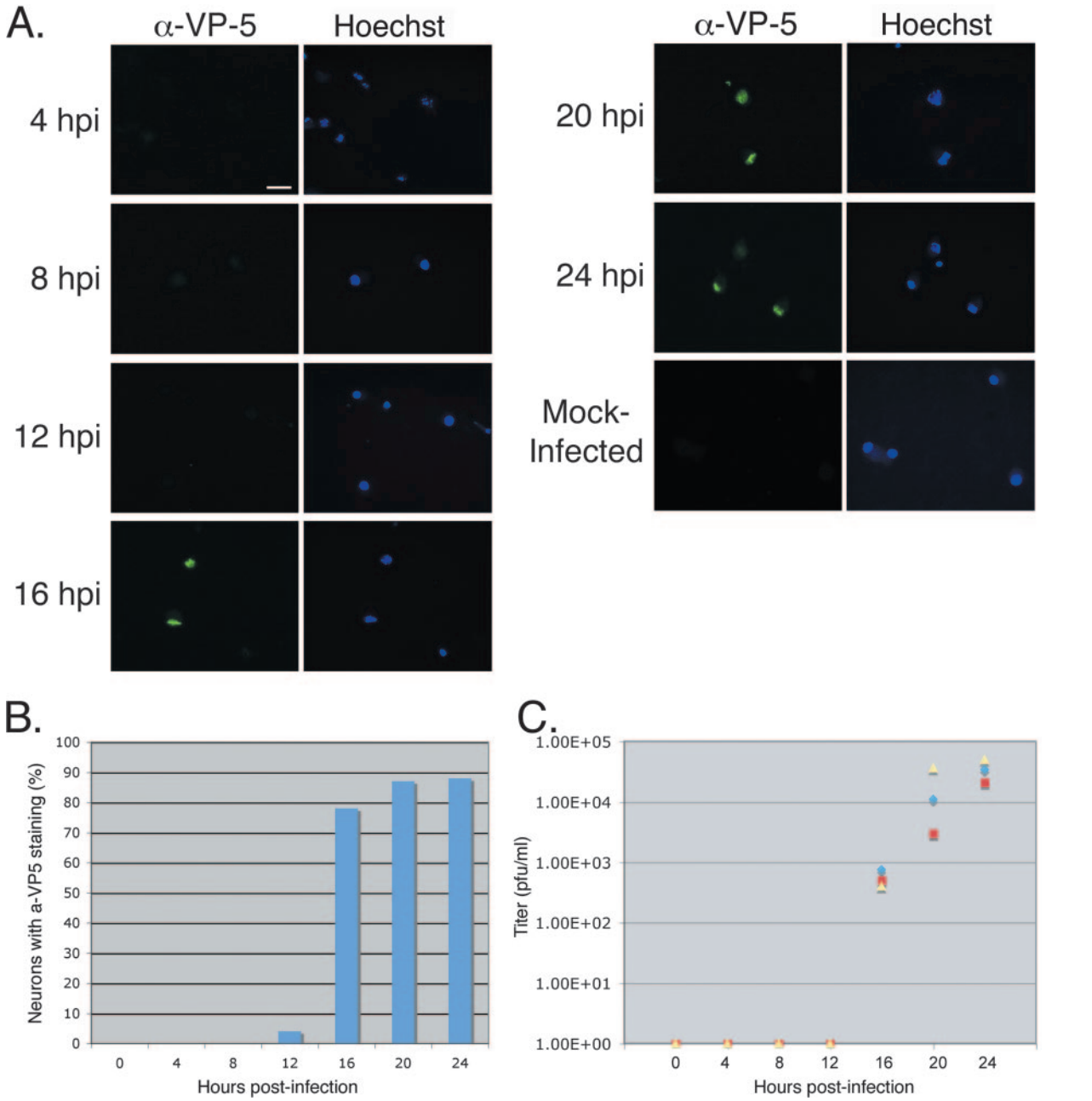

FIG. 5. Time course for in vitro transneuronal spread. Explants were infected with PRV Becker. (A) Wide-field images of neurons were fixed and stained with anti-VP5 (α-VP-5) antibody and Hoechst 33342 at 24 h postinfection. Only dissociated cells inside the chamber are shown. The same field of neurons is shown in the anti-VP5 panel as in the Hoechst panel. Three chambers were used for each time point. Scale bar, 20 μm. (B) Quantitation of neurons infected inside chambers. Neurons positive for anti-VP5 staining were scored as infected. (C) Quantitation of spread via titer determination. The medium in the chamber was harvested at 24 h postinfection, and the titer was determined for PRV plaques on PK15 cells. Three chambers were harvested for each time point.

ported inside vesicles (Feierbach, Bisher, and Enquist, unpublished). Taken together, our TEM data using the isolator chamber system indicate that infecting capsids in axons are not in vesicles, while newly produced capsids likely enter axons in membrane vesicles.

Live imaging of viral movements within the chamber. To study the dynamics of virion components inside the chamber, we used a previously described dually fluorescent virus encoding a gD-GFP fusion and an mRFP fusion to VP26, a capsid protein (1). For these live imaging experiments, we cultured the chambers on glass-bottom dishes (see Materials and Methods). We infected outside the chamber with the dual-fluorescent virus and began imaging virions within axons inside the chamber at approximately 15 h postinfection. We chose 15 h postinfection based on the kinetics of infection in the chamber system as determined above. At this time point, the puncta

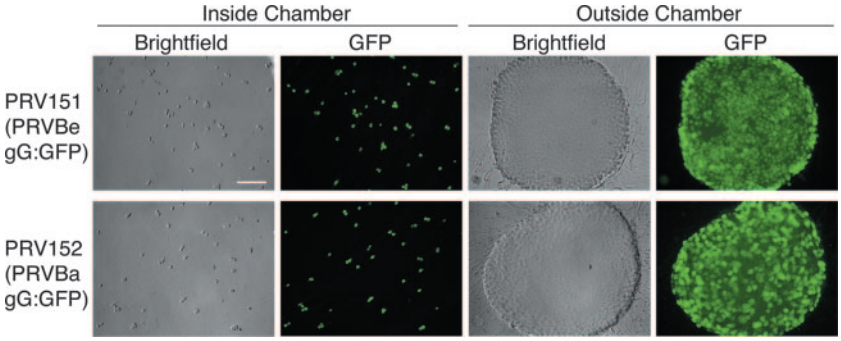

FIG. 6. Retrograde transneuronal spread of PRV in the isolator chamber system. The dissociated SCG neurons inside the ring were infected with PRV151 (a Becker recombinant expressing GFP) or PRV152 (a Bartha recombinant expressing GFP) and fixed at 24 h postinfection. Wide-field images of neurons inside the chamber and explants outside the chamber and bright-field and corresponding GFP images are shown. Scale bar, 150 μm.

were largely of two classes: green and yellow (Fig. 8A and see Movie S1 in the supplemental material). The green particles are presumably gD-GFP-positive vesicles, but without capsids. The yellow puncta were overlapping red and green fluorescence, indicating the presence of both gD-GFP and mRFP-VP26. We also imaged red fluorescent puncta without green, suggesting that these may be capsids without an envelope, although small quantities of green fluorescence may be below our detection limit. In the axons within the chamber, the green and yellow particles largely traveled in the direction opposite from that of the red particles, sometimes crossing paths within the same axon (Fig. 8B).

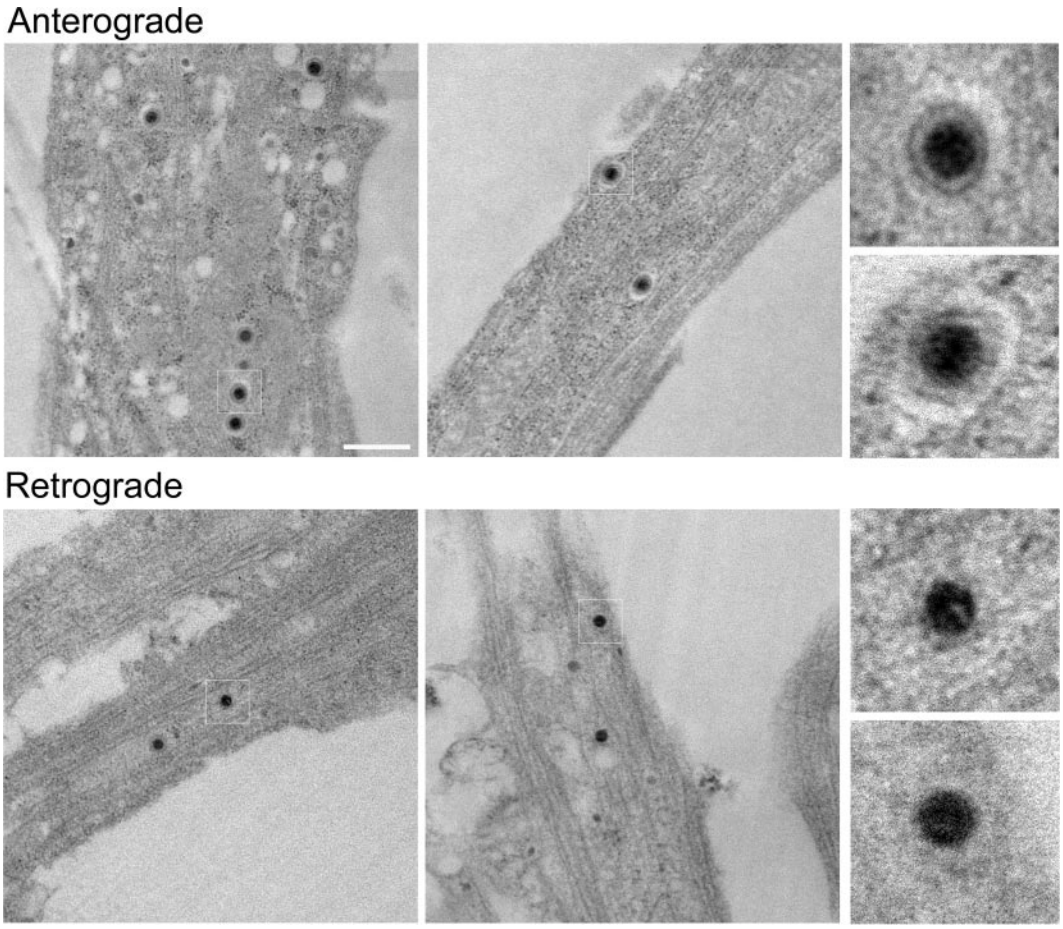

FIG. 7. TEM of virus particles during anterograde or retrograde spread. Electron micrographs of axons inside the chamber (top row) show that viral capsids are enclosed in vesicles during anterograde spread. Electron micrographs of axons located between the explant and the chamber ring (bottom row) show that viral capsids are not enclosed in vesicles during retrograde spread. Scale bar, 500 nm.

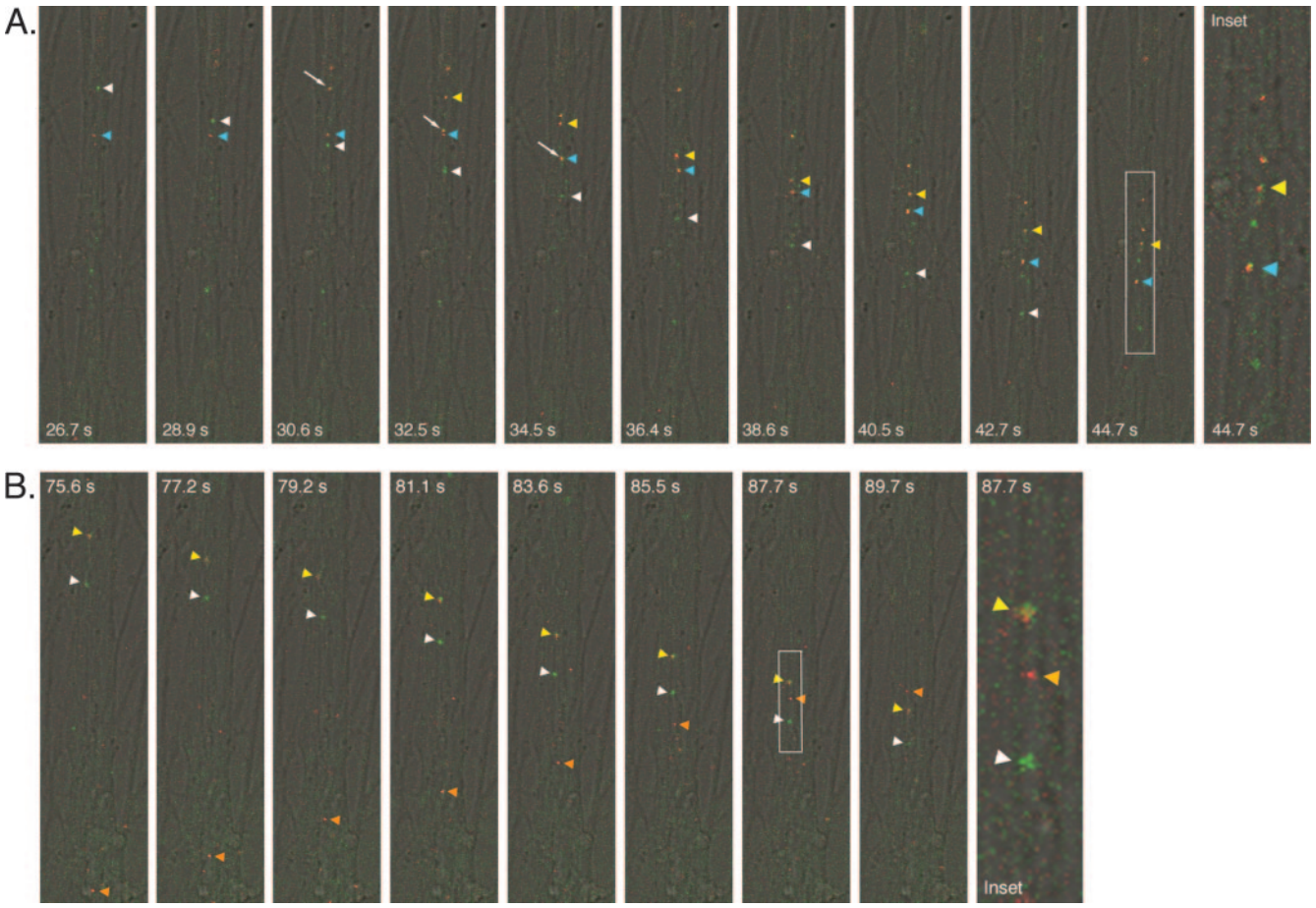

FIG. 8. Live imaging of virion component dynamics within the isolator chamber using the Leica SP5 confocal microscope. The explant outside the ring was infected with PRV expressing a mRFP-capsid fusion and a gD-GFP fusion. The axons inside the ring run along the longitudinal axis of the frame and were imaged approximately 15.5 h postinfection. The ring edge and explant are located just beyond the top of the frame. The time scale shown at the bottom of each panel is synchronous with Movie S1 in the supplemental material. Figure insets are zoom images of the white outlined areas and refer to the time points indicated. (A). A gD-positive punctum (white arrowhead) crosses paths with a stationary punctum (blue arrowhead). The stationary particle "combines" with the yellow punctum (white arrow), and they proceed together. (B) A red fluorescent punctum (orange arrowhead) moves in the opposite direction from a gD-positive punctum and a yellow punctum and eventually crosses their path in the same axon.

We also imaged virion component dynamics adjacent to and within neuronal cell bodies within the chamber (see Movie S2 in the supplemental material). These cell bodies inside the chamber become infected only after the infection has spread via anterograde transport in axons from cell bodies in the explant outside the chamber. Thus, we are imaging second-order-infected neurons. We see robust infection in these postsynaptic neurons between 16 and 18 h postinfection. Each neuronal cell body possessed at least one axon, with many having three or more. At this point, we do not know unequivocally which axons belong to the cell bodies versus those coming from the explant. However, morphological indications such as axon hillocks (the widened area at the top of an axon at the cell body) serve as good indicators of axons that belong to an individual cell body. For example, the cell body in Fig. 9 likely has three axons (two axons projecting from the top and one at the bottom [Fig. 9A, white arrows]). We imaged virion components within all three of these axons. Within the axon at the bottom, we imaged the retrograde movements of red puncta towards the cell body and could track their movements as they entered the cell (Fig. 9A). The axon at the bottom faces the center of the ring, suggesting that these capsids are undergoing retrograde spread from another neuron within the ring. We also tracked the movement of a yellow particle entering into the same cell 3 min later (Fig. 9B). However, this yellow particle did not appear to be traveling in one of the three axons of the cell body. Instead, this particle may be entering in an anterograde manner from an axon emanating from the explant or from another dissociated neuron.

DISCUSSION

In this report, we describe the neuron-to-neuron spread of alphaherpesvirus infection using SCG neuron explants cultured outside a Teflon ring containing SCG-dissociated neurons. We demonstrated spread of infection from explant neurons outside the chamber to dissociated neurons inside the isolator chamber (anterograde spread, Fig. 1 to 5 and 7) and

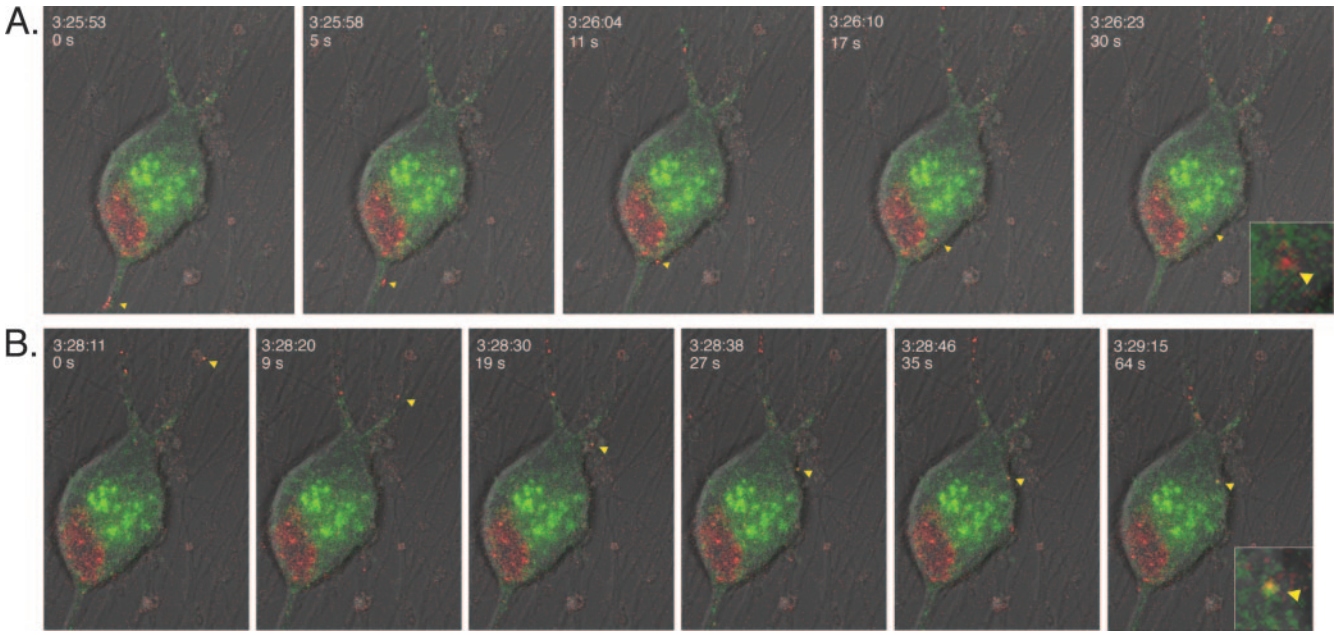

FIG. 9. Live imaging of virion component dynamics entering postsynaptic cells inside the isolator chamber using the Leica SP5 confocal microscope. The explant outside the ring was infected with PRV expressing a mRFP-capsid fusion and a gD-GFP fusion. White arrows in first frame indicate putative axons emanating from the cell body shown. The area inside the cell body that is RFP positive is the nucleus. The majority of the axons are running along the diagonal from the top right to the bottom left and were imaged approximately 17.5 h postinfection. The explant and the ring edge are located beyond the top right of the frame. The time scale shown is the time in which the experiment was conducted and is synchronous with Movie S2 in the supplemental material. The time in seconds from the first frame is also shown. Insets are zoom images of the particles indicated by arrows. (A) Entry of a red punctum (yellow arrowhead) into the cell body. (B) Entry of a yellow punctum (yellow arrowhead) into the same cell body approximately 2 min later.

vice versa (retrograde spread, Fig. 6 and 7). PRV transneuronal spread requires intact axons (Fig. 3) and the presence of gE, gI, and Us9 proteins (Fig. 4) and is not mediated by gD (Fig. 4). In addition, such spread requires the essential membrane protein gB (Fig. 4). In this system, transneuronal spread is rapid and relatively synchronous (Fig. 5). We exploited the physical isolation of primary and secondary neurons by the chamber to demonstrate ultrastructural differences in capsids during axonal infection and egress (Fig. 7). Similarly, we used live imaging technology to visualize virion components as they trafficked from explants to neurons within the chamber (Fig. 8 and 9). The ability to image axons physically isolated from the site of infection removes ambiguity from identifying input virions from newly made particles. By all these criteria, transneuronal spread in vitro faithfully recapitulates previous in vivo studies. This isolator chamber system not only provides a facile surrogate for animal infection studies but also enables several modalities of analysis, including classical virology and imaging technology. While we used pure neuronal cultures, it is possible to use mixed cultures to approximate complex tissues such as central nervous system neurons, epithelial cells, and immune cells (unpublished observations).

Previous chamber systems were developed to study viral spread from neurons to epithelial cells (6, 8, 13, 17, 19, 20, 25, 29). The isolator chamber system offers particular advantages over these classic Campenot chambers. First, the isolator chamber is placed on top of preexisting axons emanating from the explant. This step is in contrast to the other chamber systems that require axon penetration under the chamber, a step requiring etching of guidance grooves on the culturing surface. These grooves can lead to leaks that compromise the integrity of the isolating chambers. Because in our system, the chamber is gently sealed upon preexisting axons, the inefficiency of axonal penetration under the barrier is removed. Second, since axon guidance grooves are not required, glass surfaces can be used, facilitating live imaging. Third, a second population of neurons can be cultured and contained inside the chamber, which offers a particular advantage. The axons from these neurons will grow to the chamber wall, but in the absence of guidance grooves, do not penetrate under the barrier and stay completely within the ring. Therefore, neurons inside the chamber cannot form contacts with neurons outside the chamber, allowing for the unambiguous study of directional transneuronal spread.

We used the system to confirm the transneuronal properties determined in other systems. In every case, our results are consistent with those from animal models. For example, using a PRV gD null mutant, we verified that gD is not required in transneuronal spread of PRV infection. PRV gD is an essential viral ligand required for entry and fusion of extracellular virions to cells by binding various receptors, including herpesvirus entry mediator, nectin-1, and nectin-2 (31). We also verified that PRV gB is required absolutely for transneuronal spread of infection. PRV gB is an essential glycoprotein that is part of the core membrane fusion complex of gB/gH/gL and is required for transmission of infection either by extracellular particles or by cell-to-cell spread.

The finding that gD is required for the entry of extracellular

particles into cells, but not for transneuronal spread, suggests two possible models: (i) mature extracellular virions are not involved in transneuronal spread, or (ii) extracellular virions use gD-independent receptors to gain entry into postsynaptic cells. Viral infection may lead to fusion of membranes between pre- and postsynaptic neurons, possibly at the synapse due to closely opposed membranes. Membrane fusion would create a continuous cytoplasm, which would allow an infection to pass from neuron-to-neuron without involving an extracellular particle. Our preliminary live imaging experiments revealed the apparent entry of a yellow particle into a postsynaptic cell (Fig. 9B). More work is needed to understand how such entry is achieved.

The isolator chamber system is readily amenable to studies of directional transneuronal spread, as demonstrated by the studies with PRV Bartha infections. We verified that PRV Bartha fails to spread in the anterograde direction (from explant neurons to neurons within the chamber) but spreads readily in the retrograde direction (from neurons within the chamber to explant neurons) (compare Fig. 4 with Fig. 6).

The isolation chamber offers the possibility of examining axons physically separated from the site of infection by live optical imaging techniques as well as TEM. This property circumvents potentially confounding issues such as endocytosis of input virions and release of progeny virions followed by reinfection. We observed by TEM that progeny capsids that assembled in the cell body and sorted into axons were in membrane vesicles. These structures were observed in mid-axon and were not adjacent to varicosities. We conclude that during viral egress, PRV capsids enter axons and are transported in cellular membranes. In contrast, when we infected inside the chamber and examined the explant axons outside the chamber, capsids were not contained within a membrane. These capsids were surrounded by a halo of electron-dense material, most likely tegument proteins. Consistent with these two lines of study, Antinone et al. found using time-lapse fluorescence imaging of living primary neurons that capsids colocalize with the membrane protein gD during anterograde transport, indicating capsid association with a membrane (1). In contrast, when the capsids were traveling in the retrograde direction shortly following entry, capsids were rarely found associated with gD (1).

We conducted live imaging of fluorescently labeled viral particles inside the chamber, which separates the site of infection from the site being imaged. Similar to previous live imaging studies, we found that viral particles moved in both anterograde and retrograde directions (1, 30). Our study confirms that of Antinone et al., observing that capsids (red fluorescence) and gD (green fluorescence) travel together (shown by yellow fluorescence). Because the Leica SP5 confocal laser lines excite GFP and RFP simultaneously, we were able to capture the green and red channels at the same time, giving rise to yellow puncta when the images were merged. At early imaging time points prior to replication inside the ring, the yellow particles only moved in one direction—away from the explant. Thus, these particles are likely moving in the anterograde direction. This is consistent with our finding that capsids traveling in the anterograde direction are surrounded by an envelope (Fig. 7) and that of Antinone et al. demonstrating that red puncta (capsids) traveling in the anterograde direction contain gD (1). We also imaged red puncta (capsids) traveling in the opposite, presumably retrograde, direction—sometimes in the same axons as yellow particles. We do not yet know the nature of these red puncta in that they could be capsids that separated from gD and reversed direction or capsids that are traveling retrograde postreplication (as observed by Antinone et al.). It is likely that this population of capsids is a result of both events.

Virion components tagged with fluorescent proteins are dynamic in infected neurons inside the ring. In contrast to capturing movements of virion components in axons where a single confocal optical slice is imaged, when imaging cell bodies, we acquired 3D stacks over time to gain more spatial information. Using this method, we were able to see the entry of both red and yellow fluorescent puncta into cell bodies. Interestingly, the yellow puncta shown in Fig. 9 did not appear to enter the cell body within one of its own axons—raising the possibility that we have captured transneuronal spread. If this is indeed the case, then it may be that the particle has entered into the postsynaptic neuron accompanied by its envelope. Without a live synaptic marker, it is impossible to know if this particle entered the neuron via a synapse.

The development of the in vitro isolator chamber system is a key step in elucidating the molecular mechanisms of viral spread between neurons, as we now can begin to dissect the host cell requirements for viral spread. Neural circuit-tracing experiments in vivo have shown that alphaherpesviruses spread only between synaptically connected neurons in a circuit (reviewed in references 10 and 11). One mechanism for spread involves the virus engaging host presynaptic (or postsynaptic) complexes to facilitate spread via synapses. Another mechanism would be that close apposition of membranes such as tight junctions would facilitate spread. A study of PRV spread between neurons and epithelial cells in the trichamber system has shown that the infection spreads from axons to clusters of epithelial cells at discrete sites along the axon. At these sites, both virus and the lipophilic dye DiI spread from the axons to the epithelial cells, indicating that these are sites of contact and perhaps even membrane fusion (6). A recent paper from De Regge et al. has demonstrated that PRV infection triggers the formation of presynaptic terminals along axons via gD binding to host nectin (9). These authors have also shown that such terminals serve as virus exit sites (9). Thus, alphaherpesviruses may be able to induce the formation of additional sites of egress to more efficiently facilitate spread from axons.

This chamber system enables us to determine the physical nature of the entity that actually spreads between neurons. Is it a mature virion or some other form of an assembling virion? The live imaging of a variety of viral fluorescent fusion proteins that assemble into virion structural components will be key to determining which viral proteins spread to the next cell during directional spread (anterograde versus retrograde). Importantly, the chambers can be easily modified for electrophysiological studies of viral neuron-to-neuron spread as well as for pharmacological studies involving screening for inhibitors of axonally mediated infection, egress, and transneuronal spread.

ACKNOWLEDGMENTS

We appreciate the input and advice from members of the Enquist lab, especially Toh Hean Ch'ng, for inspiring this work. We are grate-

ful to Silvia Piccinotti for her schematic of the isolator chamber system. We thank the Schwarzbauer and Burdine labs at Princeton University for generous usage of their microscopes. We are grateful to Greg Smith (Northwestern University) for providing us with the dual fluorescent PRV strain. We thank Alex Flood for development of the anti-VP5 antibody. Special thanks goes to Robert Pelham for his continued care and support throughout this study.

This work was supported by the National Institute of Neurological Disorders and Stroke (NIH-NINDS; grant R01 33506) and the Dana Research Foundation.

REFERENCES

1. **Antinone, S. E., and G. A. Smith.** 2006. Two modes of herpesvirus trafficking in neurons: membrane acquisition directs motion. J. Virol. **80:**11235–11240.
2. **Babic, N., T. C. Mettenleiter, A. Flamand, and G. Ugolini.** 1993. Role of essential glycoproteins gII and gp50 in transneuronal transfer of pseudorabies virus from the hypoglossal nerves of mice. J. Virol. **67:**4421–4426.
3. **Banker, G., and K. Goslin.** 1991. Culturing nerve cells. MIT Press, Cambridge, MA.
4. **Campenot, R. B.** 1982. Development of sympathetic neurons in compartmentalized cultures. II. Local control of neurite survival by nerve growth factor. Dev. Biol. **93:**13–21.
5. **Ch'ng, T.-H., E. A. Flood, and L. W. Enquist.** 2004. Culturing primary and transformed neuronal cells for studying pseudorabies virus infection. Humana Press, Totowa, NJ.
6. **Ch'ng, T. H., and L. W. Enquist.** 2006. An in vitro system to study transneuronal spread of pseudorabies virus infection. Vet. Microbiol. **113:**193–197.
7. **Demmin, G. L., A. C. Clase, J. A. Randall, L. W. Enquist, and B. W. Banfield.** 2001. Insertions in the gG gene of pseudorabies virus reduce expression of the upstream Us3 protein and inhibit cell-to-cell spread of virus infection. J. Virol. **75:**10856–10869.
8. **De Regge, N., H. W. Favoreel, K. Geenen, and H. J. Nauwynck.** 2006. A homologous in vitro model to study interactions between alphaherpesviruses and trigeminal ganglion neurons. Vet. Microbiol. **113:**251–255.
9. **De Regge, N., H. J. Nauwynck, K. Geenen, C. Krummenacher, G. H. Cohen, R. J. Eisenberg, T. C. Mettenleiter, and H. W. Favoreel.** 2006. Alpha-herpesvirus glycoprotein D interaction with sensory neurons triggers formation of varicosities that serve as virus exit sites. J. Cell Biol. **174:**267–275.
10. **Enquist, L. W.** 2002. Exploiting circuit-specific spread of pseudorabies virus in the central nervous system: insights to pathogenesis and circuit tracers. J. Infect. Dis. **186**(Suppl. 2)**:**S209–S214.
11. **Enquist, L. W., and J. P. Card.** 2003. Recent advances in the use of neurotropic viruses for circuit analysis. Curr. Opin. Neurobiol. **13:**603–606.
12. **Enquist, L. W., P. J. Husak, B. W. Banfield, and G. A. Smith.** 1998. Infection and spread of alphaherpesviruses in the nervous system. Adv. Virus Res. **51:**237–347.
13. **Holland, D. J., M. Miranda-Saksena, R. A. Boadle, P. Armati, and A. L. Cunningham.** 1999. Anterograde transport of herpes simplex virus proteins in axons of peripheral human fetal neurons: an immunoelectron microscopy study. J. Virol. **73:**8503–8511.
14. **Jons, A., and T. C. Mettenleiter.** 1997. Green fluorescent protein expressed by recombinant pseudorabies virus as an in vivo marker for viral replication. J. Virol. Methods **66:**283–292.
15. **Lomniczi, B., M. L. Blankenship, and T. Ben-Porat.** 1984. Deletions in the genomes of pseudorabies virus vaccine strains and existence of four isomers of the genomes. J. Virol. **49:**970–979.
16. **Lomniczi, B., S. Watanabe, T. Ben-Porat, and A. S. Kaplan.** 1984. Genetic basis of the neurovirulence of pseudorabies virus. J. Virol. **52:**198–205.
17. **Lycke, E., K. Kristensson, B. Svennerholm, A. Vahlne, and R. Ziegler.** 1984. Uptake and transport of herpes simplex virus in neurites of rat dorsal root ganglia cells in culture. J. Gen. Virol. **65:**55–64.
18. **Mettenleiter, T. C., N. Lukacs, and H.-J. Rziha.** 1985. Pseudorabies virus avirulent strains fail to express a major glycoprotein. J. Virol. **56:**307–311.
19. **Mikloska, Z., and A. L. Cunningham.** 2001. Alpha and gamma interferons inhibit herpes simplex virus type 1 infection and spread in epidermal cells after axonal transmission. J. Virol. **75:**11821–11826.
20. **Mikloska, Z., P. P. Sanna, and A. L. Cunningham.** 1999. Neutralizing antibodies inhibit axonal spread of herpes simplex virus type 1 to epidermal cells in vitro. J. Virol. **73:**5934–5944.
21. **Mulder, W., J. Pol, T. Kimman, G. Kok, J. Priem, and B. Peeters.** 1996. Glycoprotein D-negative pseudorabies virus can spread transneuronally via direct neuron-to-neuron transmission in its natural host, the pig, but not after additional inactivation of gE or gI. J. Virol. **70:**2191–2200.
22. **Peeters, B., N. de Wind, R. Broer, A. Gielkens, and R. Moormann.** 1992. Glycoprotein H of pseudorabies virus is essential for entry and cell-to-cell spread of the virus. J. Virol. **66:**3888–3892.
23. **Peeters, B., N. de Wind, M. Hooisma, F. Wagenaar, A. Gielkens, and R. Moormann.** 1992. Pseudorabies virus envelope glycoproteins gp50 and gII are essential for virus penetration, but only gII is involved in membrane fusion. J. Virol. **66:**894–905.
24. **Peeters, B., J. Pol, A. Gielkens, and R. Moormann.** 1993. Envelope glycoprotein gp50 of pseudorabies virus is essential for virus entry but is not required for viral spread in mice. J. Virol. **67:**170–177.
25. **Penfold, M. E., P. Armati, and A. L. Cunningham.** 1994. Axonal transport of herpes simplex virions to epidermal cells: evidence for a specialized mode of virus transport and assembly. Proc. Natl. Acad. Sci. USA **91:**6529–6533.
26. **Petrovskis, E. A., J. G. Timmins, T. M. Gierman, and L. E. Post.** 1986. Deletions in vaccine strains of pseudorabies virus and their effect on synthesis of glycoprotein gp63. J. Virol. **60:**1166–1169.
27. **Pickard, G. E., C. A. Smeraski, C. C. Tomlinson, B. W. Banfield, J. Kaufman, C. L. Wilcox, L. W. Enquist, and P. J. Sollars.** 2002. Intravitreal injection of the attenuated pseudorabies virus PRV Bartha results in infection of the hamster suprachiasmatic nucleus only by retrograde transsynaptic transport via autonomic circuits. J. Neurosci. **22:**2701–2710.
28. **Rauh, I., and T. C. Mettenleiter.** 1991. Pseudorabies virus glycoproteins gII and gp50 are essential for virus penetration. J. Virol. **65:**5348–5356.
29. **Saksena, M. M., H. Wakisaka, B. Tijono, R. A. Boadle, F. Rixon, H. Takahashi, and A. L. Cunningham.** 2006. Herpes simplex virus type 1 accumulation, envelopment, and exit in growth cones and varicosities in mid-distal regions of axons. J. Virol. **80:**3592–3606.
30. **Smith, G. A., S. P. Gross, and L. W. Enquist.** 2001. Herpesviruses use bidirectional fast-axonal transport to spread in sensory neurons. Proc. Natl. Acad. Sci. USA **98:**3466–3470.
31. **Spear, P. G.** 2004. Herpes simplex virus: receptors and ligands for cell entry. Cell Microbiol. **6:**401–410.
32. **Watson, D. H., W. C. Russell, and P. Wildy.** 1963. Electron microscopic particle counts on herpes virus using the phosphotungstate negative staining technique. Virology **19:**250–260.
33. **Whealy, M. E., J. P. Card, A. K. Robbins, J. R. Dubin, H.-J. Rziha, and L. W. Enquist.** 1993. Specific pseudorabies virus infection of the rat visual system requires both gI and gp63 glycoproteins. J. Virol. **67:**3786–3797.